J Mater Sci (2009) 44:6531–6537
DOI 10.1007/s10853-009-3598-1

MESOSTRUCTURED MATERIALS

One pot synthesis of mesostructured non-silica oxides nanocrystallites

Hangrong Chen · Jina Yan · Zhengqing Ye · Liangxia Zhang · Jianhua Gao · Jianlin Shi · Dongsheng Yan

Received: 13 October 2008 / Accepted: 14 May 2009 / Published online: 2 June 2009

Abstract Some typical worm-like mesoporous non-silica oxides, titania, zirconia, and dopants-incorporated zirconia oxides, with homogeneous nanocrystalline framework and narrow pore-size distribution have been synthesized via a facile process templated from composite surfactant of a long chain poly block copolymer combined with non-ionic alkyl-PEO surfactant (Brij56) under the hydrothermal condition. Bi- or even multi-component zirconia-based composites with further addition of other oxide compositions can also be obtained with well-defined mesoporous structure and nanocrystalline framework. These mesostructured oxides/composite oxides show high surface area, well-crystallization framework, and high thermal stability. XRD, nitrogen adsorption analysis, TEM, and EDX were used for the structural characterizations. The use of non-ionic block-copolymer surfactant is believed to be responsible for the crystallization of mesoporous framework and high thermal stability at high temperature without structural collapse.

Introduction

Nanostructured mesoporous materials are of great research interests for the potential applications as catalysts, adsorbents, chemical sensors, nanoelectronic/optical devices, etc [1–3]. Mesoporous transition metal oxides are particularly interesting owing to their unusual properties not possessed by silicates, such as unusual catalytic, magnetic, and optical properties, and so on [4, 5]. From the viewpoint of applications, the design and synthesis of non-siliceous mesoporous materials are even more significant than mesoporous silica, and much work has been done on mesoporous transition metal oxides [6–8]. However, most of the previously reported mesoporous zirconia/titania materials [6–8] presented amorphous framework, and in many cases the obtained mesoporous zirconia/titania materials subjected to the structural collapse once crystallization occur, which would greatly limit their practical applications. Very recently, Chen et al. [9] reported a thermally stable $ZrO_{2-x}(SO_4)_x$ mesoporous material via a facile post-treatment with NaCl. Here we show some typical mesostructured non-silica oxides, mesoporous zirconia, dopants-incorporated zirconia, and titania with nanocrystalline framework, being successfully synthesized via one pot synthesis procedure without post-treatment. This facile process can be expanded to synthesize other mesostructured non-silica nanocomposite oxides with high surface area, such as ceria–zirconia nanocomposite. These mesostructured non-silica oxide nanomaterials of very high thermal stability without mesostructural collapse, can find potential applications in different fields, such as catalysis and adsorptions.

Experimental

Sample preparation

A micellar solution (10–20 wt%) of Pluronic F-127 or P123 (BASF) and Brij56[C16(EO)10] (Aldrich) was prepared by

H. Chen · J. Yan · Z. Ye · L. Zhang · J. Gao · J. Shi (✉) · D. Yan
State Key Lab of High Performance Ceramics and Superfine Microstructure, Shanghai Institute of Ceramics, Chinese Academy of Sciences, Shanghai 200050, China
e-mail: jlshi@mail.sic.ac.cn

H. Chen
e-mail: hrchen@mail.sic.ac.cn

dissolving F123 and Brij56 in a certain ratio in distilled water at room temperature under stirring for more than 3 h. An appropriate amount of inorganic source, such as zirconium propoxide, or titanium isopropoxide, was added dropwise into the above solution under further stirring for 2 h. The typical weight ratios of dopants-incorporated mesoporous zirconia and pure mesoporous titania are (1–10 wt%) dopants: 1 Brij56: 1 P123: 5 zirconium propoxide: 50 H_2O and 1 Brij56: 2 F127: 5 titanium isopropoxide: 100 H_2O, respectively. The mixtures were transferred into a teflon-lined autoclave and heated at 120 °C for 24 h. The products were filtered and extracted by HCl ethanol solution with a volume ratio of 1:10 under refluxing at 50 °C for 4 h or calcination at 773 K to remove the surfactant species. Here the dopants can be the source of cerium, yttrium, titanium, lanthanum, molybdenum, etc.

La-doped mesoporous ceria–zirconia nanocomposite

A micellar solution (3–5 wt%) of Pluronic F-127 (SIGMA) was prepared by dissolving F127 in distilled water at the room temperature under stirring for more than 3 h. An

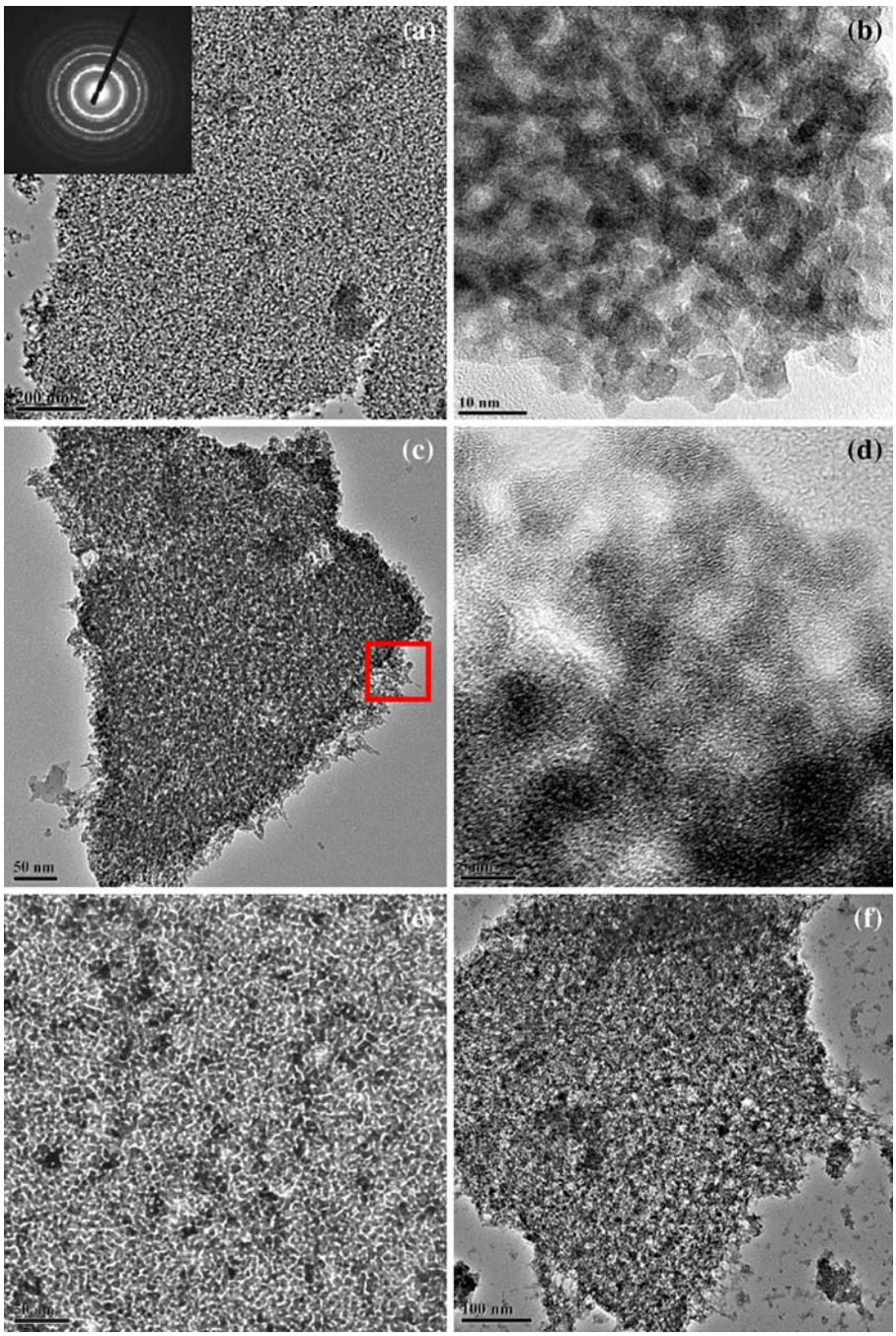

Fig. 1 Typical TEM images with different magnifications of the prepared mesostructured Mo-doped zirconia nanocrystallites after calcination at 773 K and its corresponding SAED pattern (inset) (**a**, **b**); TEM images of mesostructured Ti-doped (**c**, **d**), Y-doped (**e**), and Ce-doped (**f**) zirconia nanocrystallites

appropriate amount of ammonia (10–15 mL) was added into the above solution. Lanthanum nitrate $La(NO_3)_3$, zirconium sulfate $Zr(SO_4)_2$, and cerium(III) nitrate $Ce(NO_3)_3$ with the weight ratio of 1:6:10 was dissolved into the distilled water (50 mL) under continuous stirring. The clear aqueous solution of the inorganic salts was added dropwise into above surfactant solution under stirring for more than 4 h. The as-prepared reddish brown precipitate was transferred into a teflon-lined autoclave and heated at 393 K for 24 h. The product was washed, filtered, and calcined at different temperatures for 4 h to remove the surfactant.

Structural characterization

The XRD (X-ray Diffraction) patterns of prepared samples were recorded on a Rigaku D/Max-2200PC X-ray diffractometer with Cu target (40 kV, 40 mA). FETEM (field emission transmission electron microscopy) and EDX (energy dispersive X-ray spectroscopy) analyses were conducted with a JEOL 200CX electron microscope operated at 200 keV. BET (Brunauer-Emmet-Teller) surface area and size distributions were obtained at 77.35 K on a Micromeritics Tristar 3000 analyzer.

Results and discussion

Figure 1 shows the representative TEM images of the prepared zirconia samples with small amount of dopants, such as molybdenum, and the corresponding selected area electron diffraction pattern (SAED) (inset). The existence of the homogeneously distributed worm-like mesopores can be clearly observed, which is consistent with the N_2-sorption analysis. The SAED pattern reveals that such mesoporous zirconia has the stable tetragonal phase, in agreement with the XRD results. Figure 1b and d with much higher magnifications confirm more clearly the nanocrystalline framework as well as the mesoporous distributions.

Small amount of dopants, such as Mo, Ti, Y, Ce, can be successfully incorporated into zirconia framework without destruction of the mesoporous structure, as can be confirmed by the corresponding EDX spectra in Fig. 2. Some kinds of defects, such as oxygen vacancies and/or acidity centers, can be produced when small amount of dopants are incorporated into zirconia lattices, which is helpful to increase the active centers and enhance its catalytic performances. It is shown that up to 10 wt% dopants can be well incorporated into zirconia framework, and no separate phase of the doped oxides exist in the pores or on the outer surface of the mesoporous material.

The wide-angle X-ray diffraction (XRD) pattern of the calcined sample in Fig. 3A(a) shows broad diffraction peaks corresponding well to the mixture phases of monoclinic (JCPDF 65-1022) and tetragonal (JCPDF 50-1089) nanocrystalline zirconia as main phases. A broad small-angle peak with *d*-value of about 8.6 nm can be distinctively observed in the inset of this figure. The XRD patterns indicate that such prepared sample possesses a certain

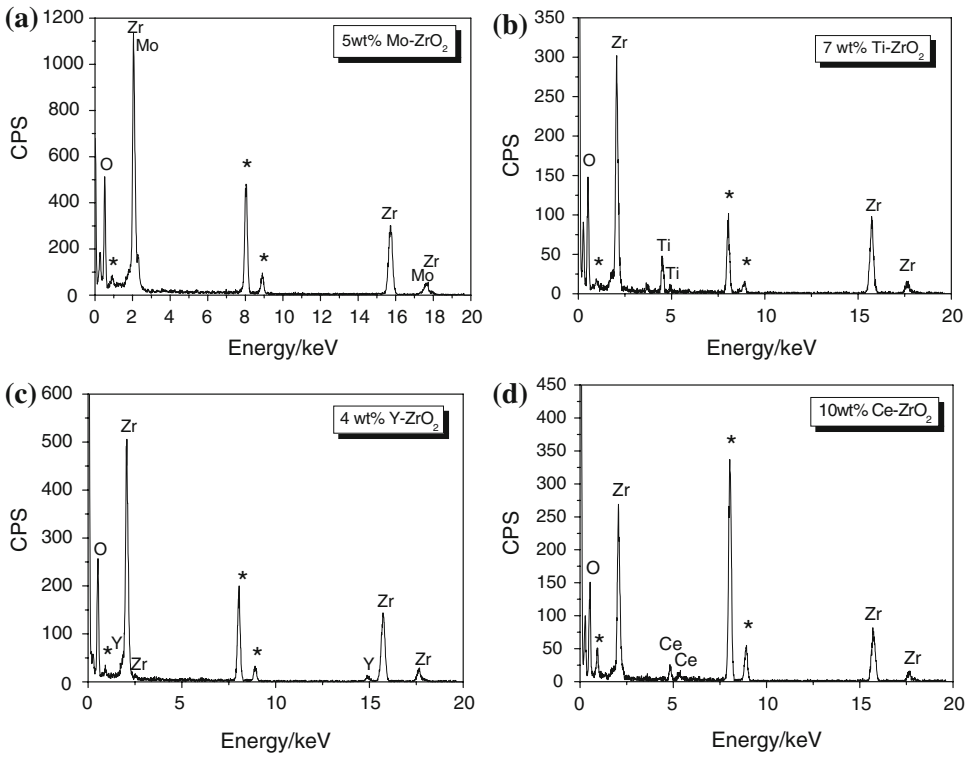

Fig. 2 Typical EDX spectra corresponding to Fig. 1(**a**, **c**, **e**, **f**), respectively

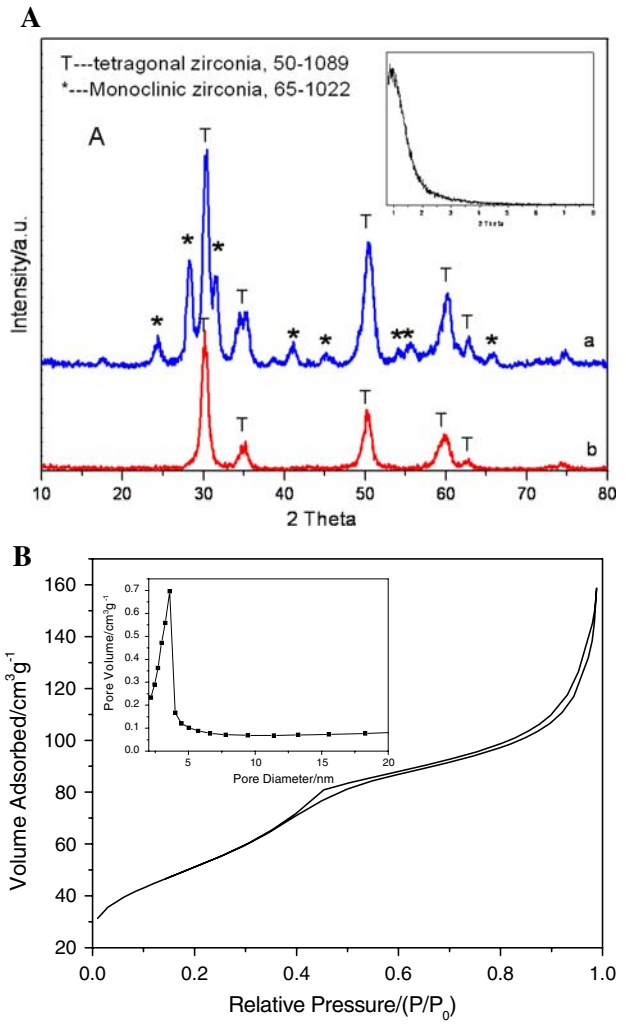

Fig. 3 **A** Typical XRD pattern of the prepared mesoporous zirconia after calcined at 773 k (a), and (b) typical XRD pattern of the same zirconia sample which was incorporated with small amount of molybdenum as reference, inset shows the low angles XRD pattern corresponding to pattern a; **B** typical N_2 adsorption-desorption isotherm and (inset) the BJH pore size distribution of the calcined sample with 5 wt% Mo dopant

degree of ordering of mesoporous structure and nanocrystalline zirconia framework after calcination at 773 K. Small amount of certain dopants, such as Mo, Y, Ce, La, etc., can be easily incorporated into the lattice of zirconia framework forming zirconia-based solid solution, which can effectively stabilize the tetragonal phase zirconia and enhance the thermal stability, as shown in the Fig. 3A(b). The average crystallite size can be calculated from the broadening of XRD peaks using Scherrer's formula. The prepared sample after calcination at 773 K shows their average crystallite sizes of around 4–5 nm.

Representative nitrogen adsorption–desorption isotherms of the calcined sample doped with 5 wt% Mo at 773 K is shown in Fig. 3B, which can be attributed to type IV, characteristic of capillary condensation in mesopores. A narrow peak in the BJH (Barrett-Joyner-Halenda) pore-size distribution curve is centered at 3.5 nm, indicative of the uniform mesopores in this material. For this prepared sample, a high BET surface area of >180 m^2/g and the total pore volume of >0.20 cm^3/g can be obtained, which is much higher than that of the ordinary zirconia under the same calcination temperature.

This preparation strategy can also be used for the synthesis of the mesoporous nanocrystalline titania. Figure 4(a, b) shows the typical TEM images of the prepared mesoporous TiO_2 with different magnifications, as well as its corresponding SAED pattern. It can be seen that the prepared titania presents well-crystalline framework composed of uniform nanocrystallites of 3–4 nm in size. The presence of mesoporous structure of narrow pore-size distribution among the nanocrystallites is clear, as further confirmed by the N_2-sorption analysis results given in Fig. 4c. The N_2 adsorption–desorption isotherms show the typical type IV isothermer, indicating the well-defined meosporous structure, and a sharp mesopores size distribution at around 4.9 nm is also clear from the inset. Such mesoporous TiO_2 has a high surface area of above 150 m^2/g for the as-prepared sample, and >100 m^2/g after calcination at 773 K.

In addition to the single component mesostructured non-silica oxides, and the non-silica oxide incorporated with small amount of individual dopant, mesostructured multi-component non-silica composite can also be successfully synthesized via this method. Figure 5(a, b) shows the typical TEM images of the prepared mesostructured La-doped CeO_2–ZrO_2 composite after calcination at 773 K, and its corresponding area of EDX spectrum is shown in Fig. 5c. It can be seen that such prepared bi-component composite well remained in the mesoporous structure and nanocrystalline framework. According to the EDX analysis, the typical composition of this composite is $La_{0.05}Ce_{0.6}Zr_{0.35}O_2$. The corresponding N_2-sorption analysis (Fig. 6) shows clearly the typical type IV isothermer and the well-confined mesostructure with narrow mesopore size distribution, further confirming the existence of the mesoporous structure. Ceria–zirconia oxides are the most widely used materials for oxygen storage/release in modern three-way catalysts (TWCs) [10], and the previous reports via chemical/microemulsion coprecipitation methods usually resulted in non-mesoporous structure [11, 12]. For the mesoporous structure with high surface area and narrow pore size distribution, small amount of noble metal particles can be easily dispersed homogeneously into the pore channels and/or surface of such nanocomposite, which can greatly enhance the catalysis performances. Furthermore, the mesostructural tri-component alumia–ceria–zirconia

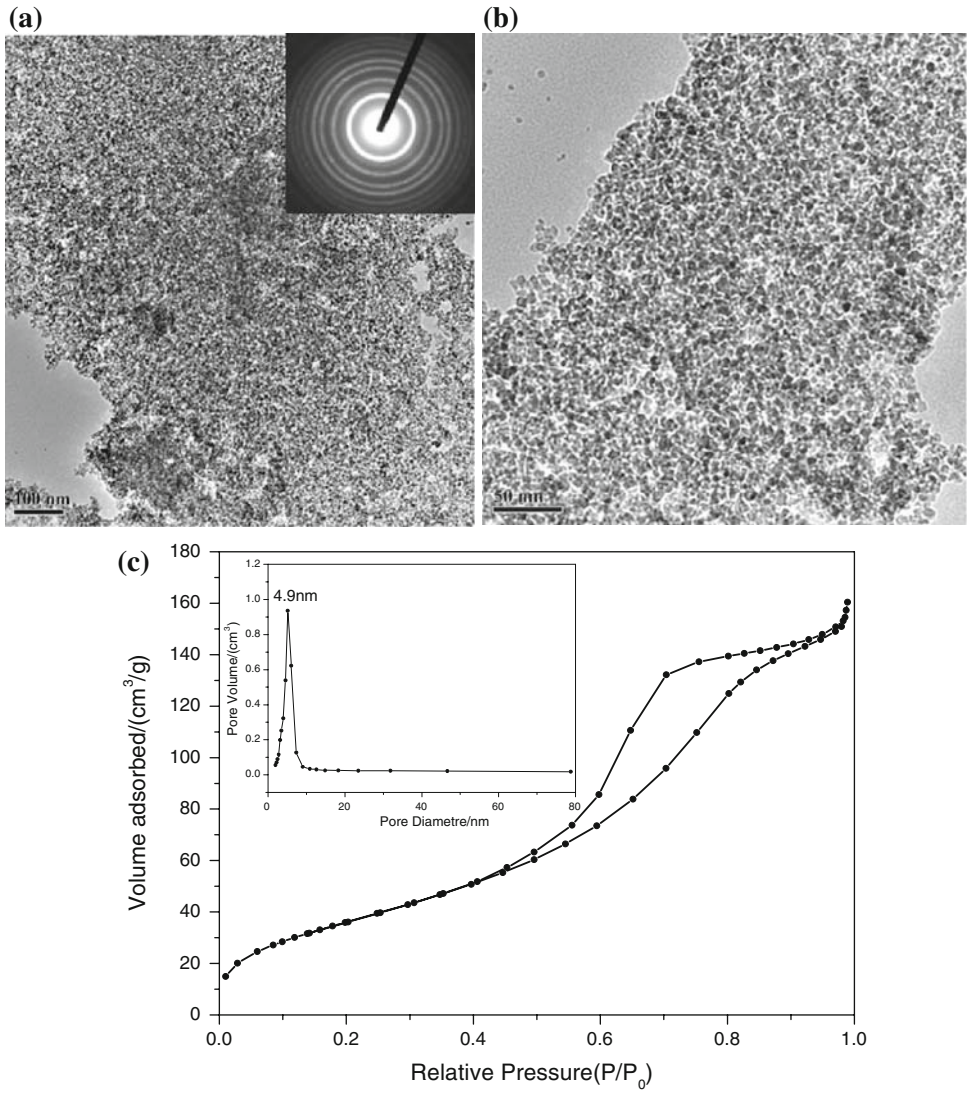

Fig. 4 (**a**, **b**) Typical TEM image of the prepared mesostructured titatia nanocrystallites and its corresponding SAED pattern (inset); **c** typical N_2 adsorption-desorption isotherm and (inset) the BJH pore size distribution of the prepared titatia sample

nanocomposite can also be obtained via a similar procedure, and such nanocomposite shows very high thermal stability. Figure 7a shows the typical TEM image of the prepared mesostructured composite Al_2O_3–CeO_2–ZrO_2 after calcination at 1273 K, and its corresponding EDX spectrum is shown in Fig. 7b. It can be seen that the mesostructure of such composite remains well even after calcination under 1273 K, indicative of high thermal stability. The corresponding EDX spectrum confirms that the presence of Al_2O_3, CeO_2, and ZrO_2 with different ratios co-exist in this mesostructural material. This mesoporous composite shows high oxygen storage capacity (OSC) (more than 400 μmol/g) and great redox properties, which can find potential applications for exhaust three-way catalysis with greatly improved aging resistance against high temperature.

The presence of non-ionic alkyl-block-copolymer surfactant plays a key role in the mesostructure formation as well as the high thermal stability. In one hand, the presence of hydrophilic alkyl-PEO surfactant in solution can lower the interface tension in the pores; thus, the growth of nanocrystallites can be slowed down. In the other hand, the homogeneous presence of surfactant molecules around the non-silica nanoparticles in solution can form a strong spatial hindrance, which generate the mesopores of around several nanometers in between crystallites and can effectively prevent nanocrystallites from strong and extensive aggregation with each other due to the long hydrophobic chains (PPO). Therefore, uniform nanocrystalline mesoporous framework can be achieved and in the meantime the fast crystallite growth can be inhibited during hydrothermal treatment. In addition, it is noticed that there are three

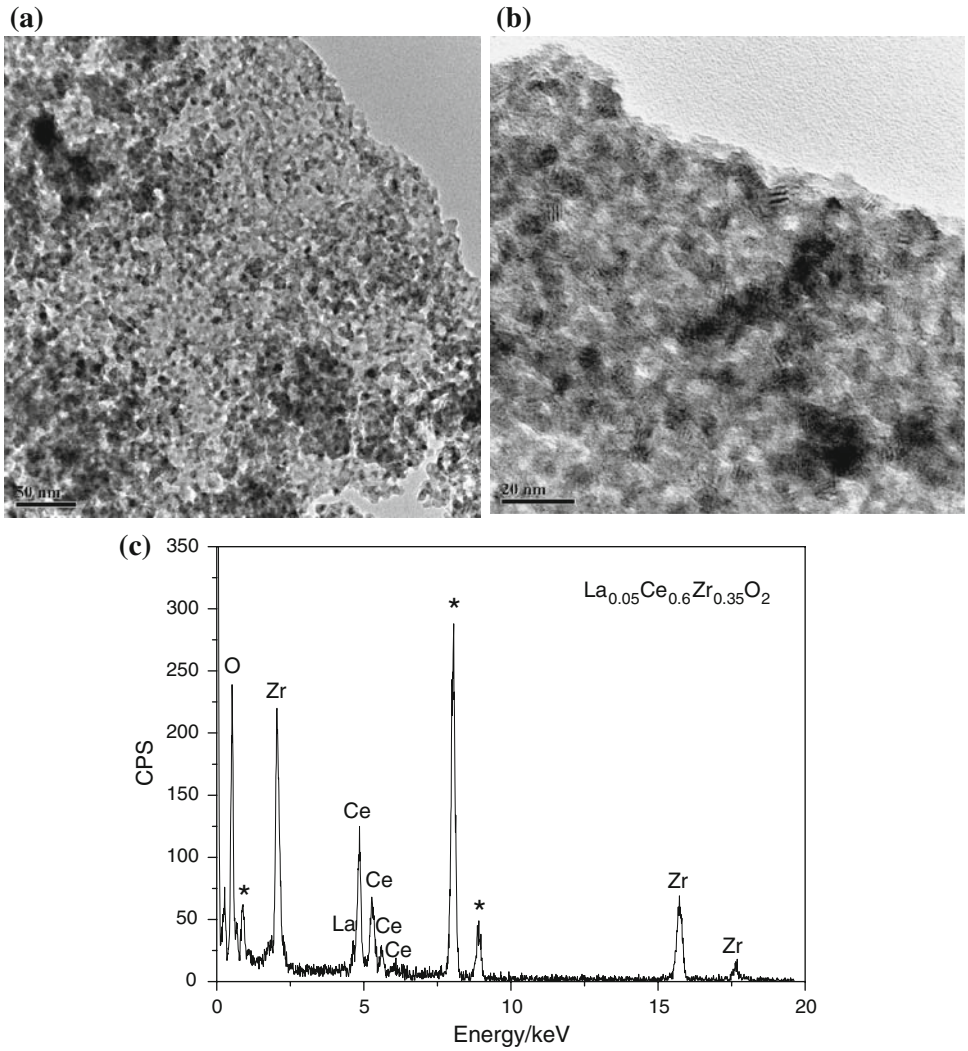

Fig. 5 **a**, **b** Typical TEM images of the prepared mesostructured La-doped CeO_2–ZrO_2 nanocomposite and **c** its corresponding EDX spectrum (* is the signal arising from the supporting Cu grid)

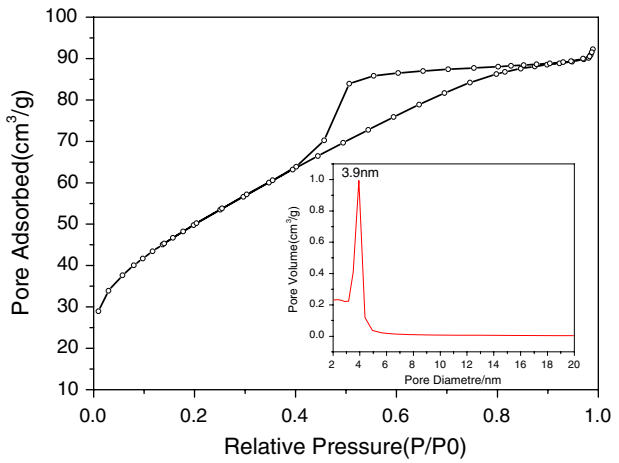

Fig. 6 Typical N_2 adsorption-desorption isotherm and (inset) the BJH pore size distribution of the prepared mesostructural CeO_2–ZrO_2 nanocomposite sample

kinds of N_2 adsorption–desorption isotherms presented by different hysteresis loops, as shown in Figs. 3B, 4c, and 6, which can be attributed to the different non-ionic alkyl-block-copolymer surfactants used in the material preparation, such as much longer hydrophobic chains of F127 than that of P123. Therefore, mesoporous structure of the synthesized sample can be easily controlled by adjusting the different kinds of surfactants.

High thermal stability of the prepared mesoporous non-silica oxides/composites against aging during calcination at temperatures from 773 to 1273 K can be attributed to the uniform mesostructure of the prepared materials due to the application of such copolymer surfactant. In the mesostructure, nanocrystallites of the framework possess uniform crystallite size and high dispersion; therefore, the driving force for the crystallize growth is greatly diminished.

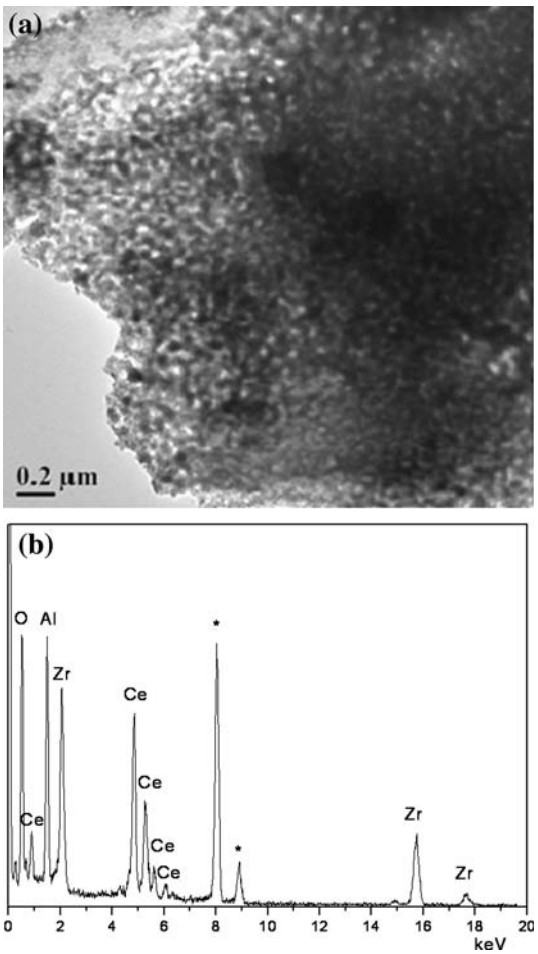

Fig. 7 **a** Typical TEM image of the prepared mesostructured Al_2O_3–CeO_2–ZrO_2 nanocomposite after calcination at 1273 K, and **b** its corresponding EDX spectrum (* is the signal arising from the supporting Cu grid)

Acknowledgements We gratefully acknowledge the financial support from the National Natural Science Foundation of China with Contract 50872140, the State Scientific & Technological Supporting Project (2007BAJ03B01), and Shanghai standard project (08DZ0 5020000).

References

1. Scott BJ, Wirnsberger G, Stucky GD (2001) Chem Mater 13:3140
2. Shi J, Hua Z, Zhang L (2004) J Mater Chem 14(5):795
3. Trong On D, Desplantier-Giscard D, Danumah C, Kaliaguine S (2001) Appl Catal A Gen 222:299
4. Dong X, Chen H, Zhao W, Li X, Shi J (2007) Chem Mater 19:3484
5. Ying JY, Mehnert CP, Wong MS (1999) Angew Chem Int Ed 38:56
6. Kim A, Bruinsma P, Chen Y, Wang L-Q, Liu J (1997) Chem Commun 161
7. Antonelli DM (1999) Adv Mater 11:487
8. Antonelli DM (1999) Microporous Mesoporous Mater 30:315
9. Chen SY, Jang LY, Cheng S (2006) J Phys Chem B 110(24):11761
10. Ozawa M (1998) J Alloys Compd 275:886
11. Gonzalez-Velasco JR, Gutierrez-Ortiz MA, Marc JL, Botas JA, Gonzalez-Marcos MP, Blanchard G (2003) Ind Eng Chem Res 42:311
12. Fernández-García M, Martínez-Arias A, Iglesias-Juez A, Belver C, Hungría AB, Conesa JC, Soria J (2000) J Catal 194:385